Hindawi Publishing Corporation
Advances in Astronomy
Volume 2012, Article ID 271502, 7 pages
doi:10.1155/2012/271502

Research Article

Demography of High-Redshift AGN

Fabrizio Fiore,[1] Simonetta Puccetti,[2] and Smita Mathur[3]

[1] *Fabrizio Fiore INAF-Osservatorio Astronomico di Roma, via Frascati 33, I00040 Monteporzio Catone, Italy*
[2] *Simonetta Puccetti ASI Science Data Center, via Galileo Galilei, 00044 Frascati, Italy*
[3] *Smita Mathur Astronomy Department, Ohio State University, Columbus, OH 43210, USA*

Correspondence should be addressed to Fabrizio Fiore, fiore@oa-roma.inaf.it

Received 21 September 2011; Accepted 9 November 2011

Academic Editor: Angela Bongiorno

High-redshift AGN holds the key to understanding early structure formation and to probe the Universe during its infancy. We review the latest searches for high-z AGN in the deepest X-ray field so far, the Chandra Deep Field South (CDFS) 4 Msecond exposure. We do not confirm the positive detection of a signal in the stacked Chandra images at the position of $z \sim 6$ galaxies recently reported by Treister and collaborators (2011). We present $z > 3$ X-ray sources number counts in the 0.5–2 keV band, obtained joining CDFS faint detections (see Fiore et al. (2011)), with Chandra-COSMOS and XMM-COSMOS detections. We use these number counts to make predictions for surveys with three mission concepts: Athena, WFXT, and a Super-Chandra.

1. Introduction

The study of high-redshift AGN holds the key to understanding early structure formation and probing the Universe during its infancy. There are fundamental issues that can be tackled by studying high-z AGN (1) the evolution of the correlations between the black hole mass and the galaxy properties (see, e.g., [1] and references therein); (2) the AGN contribution to the reionization and to the heating of the Intergalactic medium and its effect on structure formation (e.g., [2, 3] and references therein); (3) scenarios for the formation of the black hole (BH) seeds that will eventually grow up to form the supermassive black holes (SMBHs) seen in most galaxy bulges (e.g., [4]); (4) we can investigate the physics of accretion at high-z. One open question is whether BH growth is mainly due to relatively few accretion episodes, as predicted in hierarchical scenarios (see, e.g., [5] and references therein) or by the so-called chaotic accretion (hundreds to thousands of small accretion episodes, [6]). The two scenarios predict different BH spin distributions, and thus different distributions for the radiative efficiency; (5) since BHs are the structures with the fastest (exponential) growth rate, they can be used to constrain both the expansion rate of the Universe and the growth rate of the primordial perturbation at high-z, that is, competing cosmological scenarios [7, 8]; (6) since the slopes of both the high-z AGN luminosity function and the SMBH mass function strongly depend on the AGN duty cycle, their measurements can constrain this critical parameter. In turn, the AGN duty cycle holds information on the AGN triggering mechanisms. The evaluation of the evolution of the AGN duty cycle can thus help us to distinguish the competing scenarios for AGN triggering and feeding [9].

Large area optical and near infrared surveys such as the SDSS, the CFHQS, the NOAO DWFS/DLS, and the UKIDSS surveys have already been able to discover large samples of $z > 4.5$ QSOs (e.g., [10, 11]) and about 50 QSOs at $z > 5.8$ (e.g., [12–14]). The majority of these high-z AGN are broad line, unobscured, high UV rest-frame luminosity (thus high bolometric luminosity) AGN. They are likely the tips of the iceberg of the high-z AGN population. Lower bolometric luminosity and/or moderately obscured AGN can, in principle, be detected directly in current and future X-ray surveys. Dedicated searches for high-z AGN using both deep and wide area X-ray surveys and a multiband selection of suitable candidates can increase the number of high-z AGN by a factor >10. In particular, it should be possible to find hundreds rare high-z, high luminosity QSOs, in both the all sky and deep eROSITA surveys (the 0.5–2 keV flux limit of the all sky survey being the order of 10^{-14} erg/cm^2/s, while that of the deep survey, covering hundreds deg^2, should be 2-3 times deeper [15]) with a selection function much less biased

than optical surveys. To constrain the faint end of the high-z AGN luminosity function and therefore the shape of the luminosity function and of the SMBH mass function, we need to best exploit current and future deep surveys. The Chandra Deep Field South is today the *premiere* field, with its 4 Msec and 3 Msec exposures obtained by Chandra and XMM, respectively, since 1999 [16, 17]. Three different approaches have been so far applied to this field: (a) direct detection of sources in X-ray maps (e.g., [16]); (b) search for X-ray emission at the position of candidate high-z galaxies selected in the red and near infrared bands [9]; (c) stacking of X-ray counts at the position of candidate high-z galaxies [18]. Here, we review all three methods and give state of the art number counts of high-z AGN at faint fluxes. We use these number counts to predict the number of high-z AGN in possible future deep X-ray surveys. A $H_0 = 70\,\mathrm{km\,s^{-1}\,Mpc^{-1}}$, $\Omega_M = 0.3$, $\Omega_\Lambda = 0.7$ cosmology is adopted throughout.

2. Stacking Analysis of Candidate High-z Galaxies

Recently, Treister et al. [18] published a positive detection of X-ray counts in stacked Chandra images obtained adding together the X-ray counts at the position of 197 candidate high-z galaxies at $z \sim 6$ in the CDFS and CDFN [19]. They find 5σ and 6.8σ detections in the soft 0.5–2 keV and hard 2–8 keV bands. Since the 2–8 keV flux they detect is about 9 times the 0.5–2 keV flux, they infer that the majority of these faint high-z galaxies host highly obscured, Compton thick AGN. The total rest frame 2–10 keV luminosity density implied by the Treister [18] result is 1.6×10^{46} ergs/s/deg^2 at $z \sim 6$. In contrast, Fiore et al. [9] analyzed X-ray counts at the position of the same Bouwens et al. [19] $z \sim 6$ galaxies in the CDFS finding just one marginal detection. Fiore et al. [9] find that the $z \sim 6$ luminosity function can be modeled using the standard double power law shape

$$\frac{\mathrm{d}\Phi(L_\mathrm{X})}{\mathrm{d}\,\mathrm{Log}\,L_\mathrm{X}} = A\left[\left(\frac{L_\mathrm{X}}{L_*}\right)^{\gamma 1} + \left(\frac{L_\mathrm{X}}{L_*}\right)^{\gamma 2}\right]^{-1}, \quad (1)$$

with $L^* = 2 \times 10^{44}$ ergs/s, $\gamma 1 = 0.8$, and $\gamma 2 = 3.4$ (the faint end slope is not truly constrained). By integrating, this luminosity function above a luminosity of 10^{42} erg/s, one obtains a total rest frame 2–10 keV luminosity density at $z \sim 6$ of 5.6×10^{45} ergs/s/deg^2, a value ~3 times smaller than that reported by Treister et al. [18]. We investigated this discrepancy between the Treister [18] and Fiore [9] results. Once again, we considered the Bouwens et al. [19] sample of 371 candidate $z \sim 6$ galaxies in the CDFS. Some of these galaxies lies close to bright X-ray sources, identified with galaxies at a different redshift, and must therefore be excluded from the analysis. We considered two exclusion radii, one similar to that used by Treister et al. [18], that is, 22 arcsec, and another, less conservative, of 10 arcsec. In both cases, we used the new Xue et al. [16] catalog of 740 directly detected X-ray sources (it is not possible to ascertain which X-ray catalog was used by [18]). We considered sources at an offaxis angle <8 arcmin, to avoid the inclusion of sources observed with a too broad PSF. We considered only one galaxy when we find 2 or more within 2 arcsec, not to count twice the contribution from each single object. We finally excluded from the samples $z \sim 6$ galaxies closer than 2 arcsec from lower redshift galaxies brighter than zmag =25, which may emit X-rays and hence contaminate the high redshift stacks. The final samples that we consider include 210 galaxies (10 arcsec exclusion radii) and 77 galaxies (22 arcsec exclusion radii). We performed stacks of Chandra counts at the position of these galaxies in four energy bands: 0.5–2 keV, 2–7 keV, 0.8–4 keV, and 1.5–5.5 keV. The total exposure times for the two sample are $\sim 2.3 \times 10^8$ seconds (77 galaxies) and $\sim 6.3 \times 10^8$ seconds (210 galaxies). Figure 1 shows the stacked images for the two samples in the four energy bands. We do not find a significant signal at the position of the galaxies in any of these images. Table 1 gives the PSF-corrected 3σ count rate upper limits from the counts collected in boxes of 5 arcsec side (area of 100 original pixels). As a comparison, Treister et al. [18] report a count rate $3.4 \pm 0.7 \times 10^{-7}$ counts/s in the 0.5–2 keV band and $8.8 \pm 1.3 \times 10^{-7}$ counts/s in the 2–8 keV band. Our more stringent upper limits are obtained for the 210 galaxy sample in the 0.5–2 keV and 2–7 keV bands. These are, respectively, comparable and 1.5 times lower than the Treister [18] claimed detections.

We can convert our count rate upper limits to a limit to the rest frame 2–10 keV luminosity density following [18]. We find a 3σ limit of $\sim 10^{46}$ ergs/s/deg^2, lower than the [18] feature, but about twice the luminosity density estimated by Fiore et al. [9].

We recall that our analysis applies to the CDFS field alone, while the [18] result applies to the joined CDFS and CDFN area. In principle, part of the discrepancy between Treister et al. [18] and our analysis could be due to cosmic variance. However, this seems unlikely because most of the Treister sources are in the CDFS, which has an exposure twice that of the CDFN. We also recall that, for the sake of robustness, our stacking analysis is the simplest possible. First, counts at the position of galaxies are added together. Second, aperture photometry is performed on the stacked images, without any optimization for off-axis-dependent PSF. Third, background is estimated in nearby regions, and, unlike [18], no removal of positive fluctuations is performed. While this simple technique does not probably push the detection to the limit, it nevertheless produced robust result. In particular, it produced positive, valuable results in the past, when applied to samples of candidate, faint, Compton thick AGN [20, 21]. The result of our Chandra analysis of the Bouwens candidate $z > 6$ galaxies has been recently confirmed by Willott [22].

3. High-z AGN Number Counts

The analyses on the CDFS, CDFN, EGS, and COSMOS fields provide samples of individual sources detected; hence, X-ray number counts of faint high-z sources can be easily computed from these samples. Figure 2 shows $z > 3$ number counts from a compilation of surveys: the Fiore et al. [9] survey of the ERS and GOODS fields, and the Brusa et al. and Civano et al. [23, 24] XMM and Chandra surveys of the COSMOS field. Figure 2 also shows the $z \sim 6$ point from [18] and the upper limit we evaluated in the previous section from

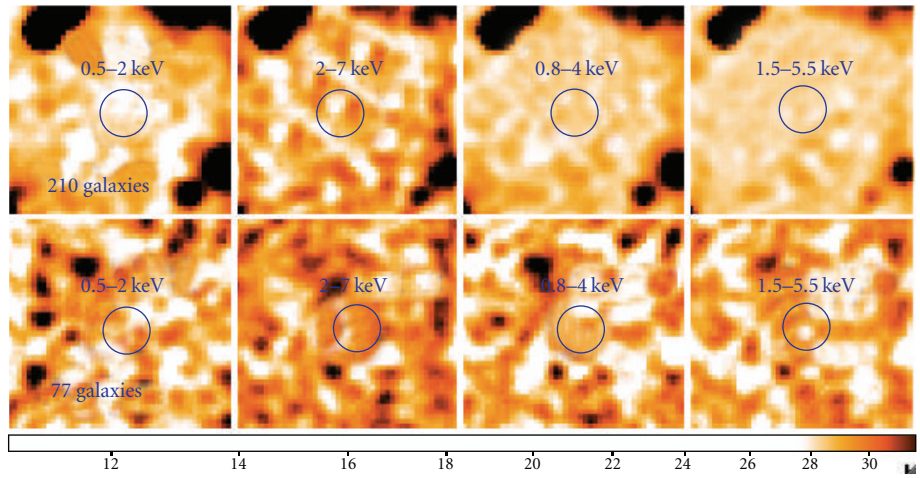

Figure 1: Stacks of Chandra images at the position of 210 and 77 Bouwens et al. [19] candidate $z \sim$ 6-7 galaxies in four energy bands: 0.5–2 keV, 2–7 keV, 0.8–4 keV, and 1.5–5.5 keV.

a stacking analysis. Black solid lines are model number counts obtained by converting the [9] luminosity functions. The model reproduces reasonably well the number counts at $z > 3$ in the full flux range probed by observations. It is consistent with the CDFS points at low fluxes in the other redshift bins, while it is slightly above the Chandra-COSMOS points at intermediate fluxes for the redshift bins $z > 4$ and $z > 5$. However, the number of sources in this survey at these redshifts is low, and the corresponding error due to both statistics and cosmic variance is large. Deeper exposures of fields with area of 1-2 deg^2 are needed to better explore this region of the redshift-flux parameter space. At the flux limits reached by the deepest Chandra exposure (4 Mseconds), there are >1000 $z > 3$ AGN/deg^2, several hundreds $z > 4$ AGN/deg^2, >100 $z > 5$ AGN/deg^2, 20–100 $z > 5.8$ AGN/deg^2 (the uncertainty on the latter number is that large, because the measure is based on just 2 candidate $z > 5.8$ galaxies detected by Chandra in the small ERS field). It is clear that, to obtain a more robust demography of the $z > 6$ AGN, a search in a much wider area, such as the CANDELS area [25], is mandatory, and requires spectroscopic confirmation of the X-ray emitting, candidate $z > 6$ galaxies. The CANDELS deep and wide surveys cover a total of 130 arcmin^2 and 670 arcmin^2 to a depth of $H = 27.8$ and $H \sim 26.5$, respectively. As a comparison, the ERS survey covers an area of 50 arcmin^2 to a depth of $H \sim 27$. The two candidate $z > 6$ ERS galaxies detected by Chandra in the ERS field are faint, $H = 26.6$ and $H = 27$ sources. The GOODS source with $z > 7$ in the Luo et al. [26] catalog has $H = 27.6$. The other $z > 6$ ERS galaxy with a marginal X-ray detection is brighter, $H = 23.8$. In summary, we expect 1–5 $z > 6$ AGN in the CANDELS deep survey and 4–20 $z > 6$ AGN in the CANDELS wide survey. We note that a fraction of these sources will be at the limit, or below, the H band sensitivity threshold of the wide survey. As of today, Chandra has spent of the order of 8 Mseconds on the CANDELS fields, most of them on the CANDELS deep fields. To reach the sensitivity to detect the faint $z > 6$ AGN in the wide area, additional 5-6 Mseconds are needed. This is within reach of the Chandra observatory in the next few years. To make further progresses with Chandra, that is, quantitatively probe the first generation of accreting SMBH, which would allow putting stringent constraints on SMBH formation models [27–30] and accretion scenarios [4–6, 31], would require to at least triple the exposure times, that is, 30–40 Mseconds dedicated to deep surveys. While this is certainly extremely expensive, it is not technically unfeasible.

Table 1: 3σ count rates upper limits.

Sample	0.5–2 keV 10^{-7} cts/s	2–7 keV 10^{-7} cts/s	0.8–4 keV 10^{-7} cts/s	1.5–5.5 keV 10^{-7} cts/s
210 galaxies	3.4	5.8	6.2	6.2
77 galaxies	5.9	9.7	9.6	10.1

4. Predictions for Future Deep Surveys

The Chandra limiting problem is that its sensitivity is very good on axis but degrades quickly at off-axis angles higher than a few arcmin, making difficult and expensive in terms of exposure time to cover with good sensitivity an area larger than a few hundred arcmin^2. A significant leap forward in the field would then be obtained by an instrument capable of reaching the Chandra Msecond on axis sensitivity (i.e., flux limit of 2–4 $\times 10^{-17}$ erg/cm^2/s), but on a factor of >10 wider field of view (FOV). We consider here three possible mission concepts, and we make predictions on the number of $z > 4$, $z > 5$ and $z > 6$ faint X-ray sources based on our best knowledge of the X-ray the number counts at high redshift (Figure 2) and of the X-ray AGN luminosity functions [9].

(1) The first mission concept that we consider is that of Athena. This is a proposal for L class mission in the framework of the ESA Cosmic Vision program. The baseline mission concept foresees an effective area for

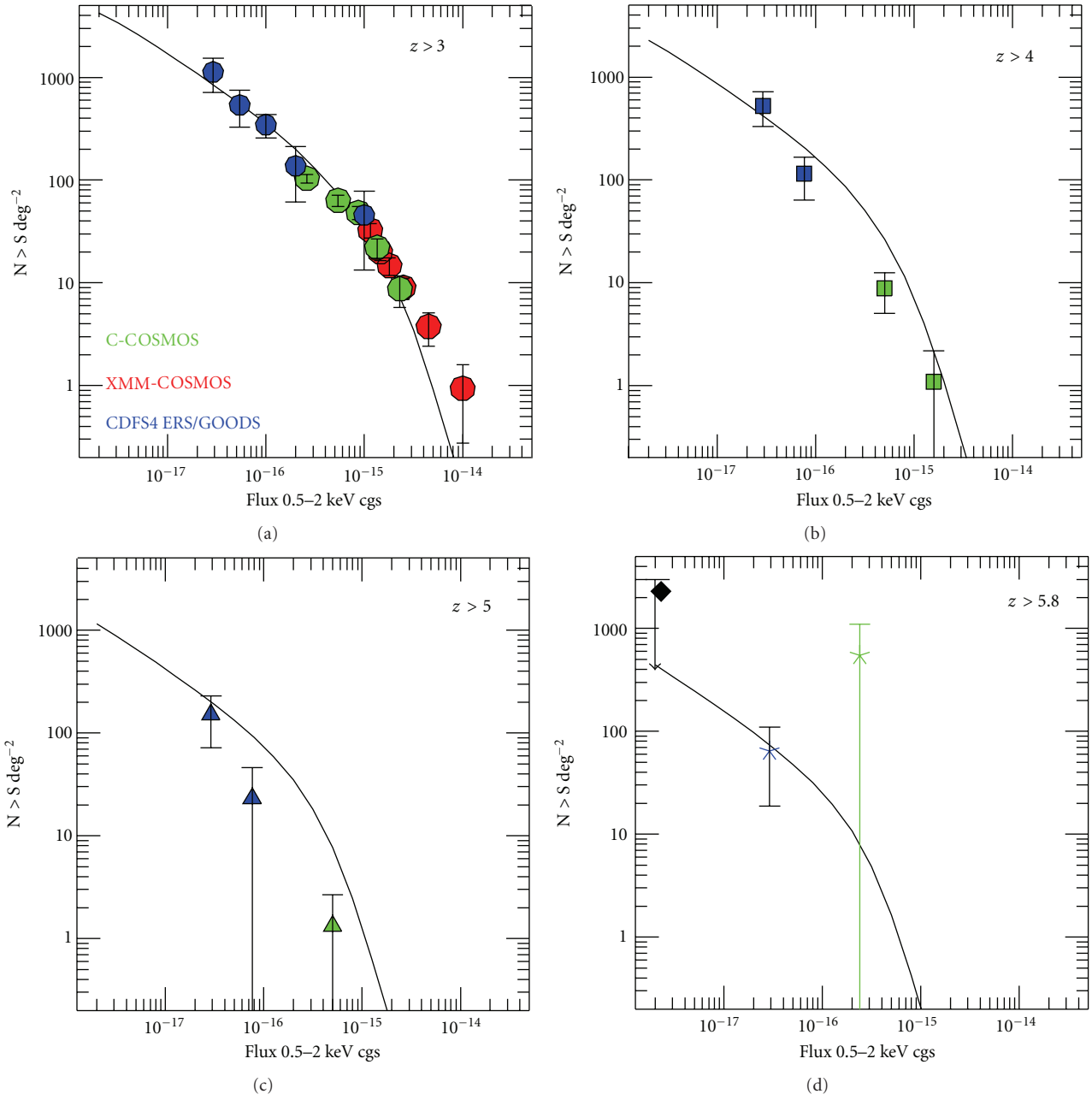

Figure 2: Faint X-ray sources number counts in the 0.5–2 keV band and in four redshift ranges. Blue points are from X-ray detections at the position of ERS and GOODS-MUSIC $z > 3$ galaxies [9]; green points are from Chandra-COSMOS [23]; red points are from XMM-COSMOS [24]. Circles = $z > 3$ sources, squares = $z > 4$ sources, triangles = $z > 5$, and star = $z > 5.8$ sources. Diamond = Treister et al. determination [18]. The upper limit in the lower right panel is from Table 1. The thin solid curves are model number counts based on the best fit high-z luminosity functions presented in [9].

imaging of the order of half square meter at 1-2 keV, a mirror PSF with half power diameter HPD ~ 10 arcsec (requirement, 5 arcsec goal), focal length 11 m, FOV = 0.17 deg^2 (25 × 25 arcmin). The observatory should be launched on a high earth orbit (HEO) or a L2 orbit, and therefore a rather high internal background is predicted, similar to the internal background measured by the instruments on board XMM and Chandra, which are flying on HEO.

(2) The second mission concept that we consider is a wide field X-ray telescope, WFXT, fully dedicated to X-ray surveys. This idea is quite old, the first proposal dating mid 90′, and the mission concept evolved considerably over the years. We assume a configuration similar to that in [32], that is an effective area of >half square meter at 1-2 keV, split in three mirror units, with HPD = 10 arcsec (requirement, goal 5 arcsec) and 5.5 m focal length. Each mirror unit is feeding

Table 2: Predicted number of faint, high-z X-ray sources.

Mission concept	PSF HPD Arcsec	Mosaics	Total FOV deg^2	z = 4-5 L_X (z = 5)	z = 5–5.8 L_X (z = 6)	z > 5.8 L_X (z = 7)
Athena*	10	60 × 0.2 Msec	10	940 > 43.3	480 > 43.5	250 > 43.6
Athena*	5	6 × 2 Msec	1.0	360 > 42.5	210 > 42.6	125 > 42.8
Athena	5	40 × 0.3 Msec	7.0	1100 > 43	650 > 43.1	360 > 43.2
WFXT*	10	24 × 0.5 Msec	24	2300 > 43.2	1300 > 43.4	600 > 43.5
WFXT*	5	4 × 3 Msec	4	1200 > 42.5	700 > 42.6	400 > 42.8
WFXT	5	60 × 0.2 Msec	60	6000 > 43.35	3200 > 43.4	1600 > 43.5
Super-Chandra	2	6 × 2 Msec	0.6	310 > 42.2	185 > 42.3	110 > 42.5
Super-Chandra	2	24 × 0.5 Msec	2.4	390 > 43	220 > 43.1	125 > 43.2
Super-Chandra	1	2 × 6 Msec	0.2	175 > 41.8	100 > 42.0	65 > 42
Super-Chandra	1	6 × 2 Msec	0.6	350 > 42.1	210 > 42.2	120 > 42.4

*Close to confusion limit (40 beams per source).

a focal plane camera with FOV ~ 1 deg^2. We assume that the observatory is in a low earth orbit (LEO), ensuring a low internal background (similar to that of the instrument on board Swift and Suzaku, which are flying on a LEO).

(3) We finally consider the concept of a Super-Chandra. This is a straw-man design for a mission with imaging capabilities comparable to Chandra (i.e., arcsec HPD), but using high throughput, light-weight mirrors (a concept pioneered by Elvis and Fabbiano some 15 years ago [33]). Good imaging capabilities using thin glass or nickel shells may be obtained by correcting the shell shape with actuators. Studies of active X-ray mirrors have been performed in the past with good results (see http://www.mssl.ucl.ac.uk/sxoptics/). A SPIE conference had been devoted to active X-ray mirrors in 2010 (proceedings of SPIE 7803). Active X-ray optics have been foreseen for extremely large throughput, subarcsec future missions like Generetion-X [34, 35] or, more recently, for a square meter, subarcsec mission (Vikhlinin et al. 2011, HEAD meeting). Here, we assume more modest throughput (~3000 cm^2 at 1-2 keV) and PSF (1-2 arcsec HPD). We also assume a limited FOV (0.1 deg^2) and a LEO, which ensures a low internal background.

We computed on axis sensitivities as a function of the observing time using the above parameters and assuming a signal to noise ratio of 3 for source detection. We assume that the effective area decreases linearly from the center to the limit of the FOV by 50% to make realistic predictions for the number of detected high-z AGN in each FOV. The background includes particle-induced internal background, as measured on HEO and LEO by Swift, Suzaku, XMM, and Chandra, cosmic X-ray background (CXB), and low temperature thermal X-ray background due to the local superbubble. To simulate the background expected for the three mission concepts, we have modified background scripts and files prepared to produce simulations for the IXO and NHXM missions. We find that the internal background dominates over the X-ray background (CXB and the local superbubble) above 0.5 keV in a HEO. Conversely, in LEO, the local superbubble dominates below 1 keV. We finally assumed a total net observing time of 12 Mseconds devoted to surveys, split in several shorther observations, to cope with source confusion and optimize the detection of $z > 5$ sources with 2–10 keV luminosity $\gtrsim 10^{42}$ ergs/s. The standard criterion for source confusion (40 beams per source) translates in a flux limit for source confusion of $\sim 6 \times 10^{-17}$ erg/cm^2/s in the 0.5–2 keV band for PSF HPD = 10 arcsec and just above 10^{-17} erg/cm^2/s for HPD = 5 arcsec. Source confusion is not an issue for any realistic exposure time for a PSF with HPD = 1 arcsec or below.

To estimate the faint X-ray sources number density, we used the model number counts in Figure 2, based on the luminosity functions presented in [9]. We conservatively assumed a flat faint-end slope of the X-ray luminosity functions, $\gamma 1 = 0.6$. Table 2 gives the predicted number of z = 4-5, z = 5–5.8, and $z > 5.8$ sources, along with their minimum 2–10 keV luminosity, for several indicative mosaics for the three mission concepts briefly described above.

It must be noted that the uncertainties on the number of sources in Table 2 is large. It is at least a factor of two at z = 4–6 and even larger at $z > 6$ (factor of 3 lower limit and a factor of 2 upper limit). The obvious message of Table 2 is that a wide field greatly helps in searching for faint high-z AGN (also see [36]). This is probably the only solution to collect samples of thousands X-ray AGN at $z > 4$. However, even a PSF as good as 5 arcsec HPD does not allow searching for sources fainter than 10^{43} ergs/s at z = 5–7. This means that only a mission with Chandra-like PSF but much higher throughput (>5 × Chandra effective area at 1-2 keV) would be able to target normal star-forming galaxies and miniquasars at z = 6-7. On one hand, a 2–10 keV luminosity of 10^{42} ergs/s at $z = 7$, reachable by extradeep exposures with a 1 arcsec PSF Super-Chandra, would be produced by a 7×10^5 SMBH emitting at its Eddington luminosity (assuming a bolometric correction of 10). Even smaller masses may be probed, if the accretion is super-Eddington. A Super-Chandra would then be able to directly search for the first generation of SMBH produced by monolithic collapse of $\gtrsim 10^5$ M$\odot$

gas clouds to BH [28–30, 37]. On the other hand, $L(2–10) = 10^{42}$ ergs/s is also produced by galaxies that form stars at a rate of $\gtrsim 200\,M_\odot$/yr ([38]). Since, at such high redshifts, the X-ray emission should mainly be due to high mass X-ray binaries, X-ray high-z galaxies could then be used to constrain the initial mass function at the epoch of galaxy formation. A Super-Chandra would then be able to open two brand-new fields in structure formation. Of course, it is not casual that the considered configuration for a Super-Chandra is able to reach these goals. Going back from scientific requirements to mission parameters, the goal of detecting sources with a 2–10 keV luminosity of $\sim 10^{42}$ at $z \sim 7$, in feasible exposure times, requires an effective area $\sim 3000\,cm^2$, given a PSF HPD $\sim$ 1 arcsec and assuming a LEO internal background.

Unfortunately a Super-Chandra is beyond the horizon of the present decade, both because of technological and programmatic issues. Furthermore, it is not clear whether a WFXT is truly feasible with such huge 1 deg^2 FOV and large throughput, and, in any case, it does not appear to be a priority in the latest US Decadal Survey (http://sites.nationalacademies.org/bpa/BPA_049810), nor in the ESA Cosmic Vision program. Conversely, Athena is a study mission for an L class mission in the framework of the ESA Cosmic Vision program. A decision on Cosmic Vision L class missions should be taken in February 2012. If positive, Athena could be implemented for the first years of the next decade. Although not reaching exquisite, Chandra-like image quality, nor extralarge field of view, Athena would be able to give a substantial contribution to the knowledge of the high-z Universe, with hundreds to a thousand $z > 4$ faint X-ray AGN (an improvement by a factor 10–100 with respect to today situation) and tens to hundreds $z > 5.8$ faint X-ray selected AGN (today, there are only 3-4 candidate $z > 6$ X-ray selected AGN in the literature [9, 26, 39], none of them spectroscopically confirmed so far).

Acknowledgments

This work was supported by ASI/INAF contracts I/024/05/0 and I/009/10/0. This work is based on observations made with NASA X-ray observatory Chandra. The authors thank the Chandra Director's office for allocating the time for these observations. X-ray data were obtained from the archive of the Chandra X-ray Observatory Center, which is operated by the Smithsonian Astrophysical Observatory.

References

[1] A. Lamastra, N. Menci, R. Maiolino, F. Fiore, and A. Merloni, "The building up of the black hole-stellar mass relation," *Monthly Notices of the Royal Astronomical Society*, vol. 405, no. 1, pp. 29–40, 2010.

[2] K. Boutsia, A. Grazian, E. Giallongo et al., "A low escape fraction of ionizing photons of $L > L^*$ Lyman break galaxies at $z = 3.3$," *The Astrophysical Journal*, vol. 736, no. 1, article 41, 2011.

[3] S. Mitra, T. R. Choudhury, and A. Ferrara, "Joint quasar-cosmic microwave background constraints on reionization history," *Monthly Notices of the Royal Astronomical Society*, vol. 419, no. 2, pp. 1480–1488, 2012.

[4] M. Volonteri and M. J. Rees, "Rapid growth of high-redshift black holes," *The Astrophysical Journal*, vol. 633, no. 2, pp. 624–629, 2005.

[5] M. Dotti, M. Volonteri, A. Perego, M. Colpi, M. Ruszkowski, and F. Haardt, "Dual black holes in merger remnants—II. Spin evolution and gravitational recoil," *Monthly Notices of the Royal Astronomical Society*, vol. 402, no. 1, pp. 682–690, 2010.

[6] A. R. King, J. E. Pringle, and J. A. Hofmann, "The evolution of black hole mass and spin in active galactic nuclei," *Monthly Notices of the Royal Astronomical Society*, vol. 385, no. 3, pp. 1621–1627, 2008.

[7] F. Fiore, "Multiwavelength perspective of AGN evolution," in *Proceedings of the International Conference on X-Ray Astronomy*, vol. 1248, pp. 373–380, 2010.

[8] A. Lamastra, N. Menci, F. Fiore, C. Di Porto, and L. Amendola, "Constraining dynamical dark energy models through the abundance of high-redshift supermassive black holes," submitted to *Monthly Notices of the Royal Astronomical Society*, http://arxiv.org/abs/1111.3800.

[9] F. Fiore, S. Puccetti, A. Grazian et al., "Faint high-redshift AGN in the *Chandra* deep field south: the evolution of the AGN luminosity function and black hole demography," *Astronomy and Astrophysics*, vol. 537, article A16, 22 pages, 2011.

[10] G. T. Richards, M. Lacy, L. J. Storrie-Lombardi et al., "Spectral energy distributions and multiwavelength selection of type 1 quasars," *The Astrophysical Journal*, vol. 166, no. 2, pp. 470–497, 2006.

[11] E. Glikman, S. G. Djorgovski, D. Stern, A. Dey, B. T. Jannuzi, and K.-S. Lee, "The faint end of the quasar luminosity function at $z \sim 4$: implications for ionization of the intergalactic medium and cosmic downsizing," *The Astrophysical Journal Letters*, vol. 728, no. 2, article L26, 2011.

[12] L. Jiang, X. Fan, F. Bian et al., "A survey of z ~ 6 quasars in the sloan digital sky survey deep stripe. II. Discovery of six quasars at $z_{AB} > 21$," *Astronomical Journal*, vol. 138, no. 1, pp. 305–311, 2009.

[13] C. J. Willott, P. Delorme, C. Reylé et al., "The Canada-France high-z quasar survey: nine new quasars and the luminosity function at redshift 6," *Astronomical Journal*, vol. 139, no. 3, pp. 906–918, 2010.

[14] D. J. Mortlock, S. J. Warren, B. P. Venemans et al., "A luminous quasar at a redshift of $z = 7.085$," *Nature*, vol. 474, no. 7353, pp. 616–619, 2011.

[15] P. Predehl, H. Böhringer, H. Brunner et al., "eROSITA on SRG," in *Proceedings of the International Conference on X-ray Astronomy*, vol. 1248, pp. 543–548, September 2009.

[16] Y. Q. Xue, B. Luo, W. N. Brandt et al., "The *Chandra* deep field-south survey: 4 Ms source catalogs," *Astrophysical Journal Supplement Series*, vol. 195, no. 1, article 10, 2011.

[17] A. Comastri, P. Ranalli, K. Iwasawa et al., "The XMM Deep survey in the CDF-S: I. First results on heavily obscured AGN," *Astronomy and Astrophysics*, vol. 526, no. 12, article L9, 2011.

[18] E. Treister, K. Schawinski, M. Volonteri, P. Natarajan, and E. Gawiser, "Black hole growth in the early Universe is self-regulated and largely hidden from view," *Nature*, vol. 474, no. 7351, pp. 356–358, 2011.

[19] R. J. Bouwens, G. D. Illingworth, J. P. Blakeslee, and M. Franx, "Galaxies at z ~ 6: the UV luminosity function and luminosity density from 506 HUDF, HUDF parallel ACS field, and goods i-dropouts," *The Astrophysical Journal*, vol. 653, no. 1 I, pp. 53–85, 2006.

[20] F. Fiore, A. Grazian, P. Santini et al., "Unveiling obscured accretion in the *Chandra* deep field-south," *The Astrophysical Journal*, vol. 672, no. 1, pp. 94–101, 2008.

[21] F. Fiore, S. Puccetti, M. Brusa et al., "Chasing highly obscured QSOs in the COSMOS field," *The Astrophysical Journal*, vol. 693, no. 1, pp. 447–462, 2009.

[22] C. J. Willott, "No evidence of obscured, accreting black holes in most $z = 6$ star-forming galaxies," *Astrophysical Journal Letters*, vol. 742, no. 1, article L8, 2011.

[23] F. Civano, M. Brusa, A. Comastri et al., "The population of high-redshift active galactic nuclei in the *Chandra*-cosmos survey," *The Astrophysical Journal*, vol. 741, no. 2, article 91, 2011.

[24] M. Brusa, A. Comastri, R. Gilli et al., "High-redshift quasars in the cosmos survey: the space density of Z > 3 X-ray selected qsos," *The Astrophysical Journal*, vol. 693, no. 1, article 8, 2009.

[25] N. A. Grogin, D. D. Kocevski, S. M. Faber et al., "Candels: the cosmic assembly near-infrared deep extragalactic legacy survey," *Astrophysical Journal Supplement Series*, vol. 197, no. 2, article 35, 2011.

[26] B. Luo, W. N. Brandt, Y. Q. Xue et al., "Identifications and photometric redshifts of the 2 Ms *Chandra* deep field-south sources," *The Astrophysical Journal*, vol. 187, no. 2, pp. 560–580, 2010.

[27] P. Madau and M. J. Rees, "Massive black holes as population III remnants," *The Astrophysical Journal*, vol. 551, no. 1, pp. L27–L30, 2001.

[28] G. Lodato and P. Natarajan, "Supermassive black hole formation during the assembly of pre-galactic discs," *Monthly Notices of the Royal Astronomical Society*, vol. 371, no. 4, pp. 1813–1823, 2006.

[29] M. Volonteri and M. C. Begelman, "Quasi-stars and the cosmic evolution of massive black holes," *Monthly Notices of the Royal Astronomical Society*, vol. 409, no. 3, pp. 1022–1032, 2010.

[30] M. C. Begelman, "Evolution of supermassive stars as a pathway to black hole formation," *Monthly Notices of the Royal Astronomical Society*, vol. 402, no. 1, pp. 673–681, 2010.

[31] N. Fanidakis, C. M. Baugh, A. J. Benson et al., "Grand unification of AGN activity in the ΛCDM cosmology," *Monthly Notices of the Royal Astronomical Society*, vol. 410, no. 1, pp. 53–74, 2011.

[32] S. Murray, R. Gilli, P. Tozzi et al., "The growth and evolution of super massive black holes," submitted to. *The Astrophysical Journal*, http://eprintweb.org/s/article/arxiv/0903.5272/.

[33] M. Elvis and G. Fabbiano, "Science driven arguments for a 10 sq.meter, 1 arcsecond X-ray telescope," *SPIE*. In press, http://arxiv.org/abs/astro-ph/9611178/.

[34] M. Elvis, R. J. Brissenden, G. Fabbiano et al., "Active X-ray optics for generation-X, the nxt high resolution X-ray observatory," *SPIE*. In press, http://arxiv.org/abs/astro-ph/0608533.

[35] S. L. O'Dell, R. J. Brissenden, W. N. Davis et al., "High-resolution x-ray telescopes," submitted to*Proceedings of the International Conference X-Ray Astronomy*, http://arxiv.org/abs/1010.4892v1/.

[36] R. Gilli, P. Tozzi, and P. Rosati, "Demography of obscured and unobscured AGN: prospects for a wide field X-ray telescope," *MemSAIT*. In press, http://arxiv.org/abs/1010.6024/.

[37] G. Lodato and P. Natarajan, "The mass function of high-redshift seed black holes," *Monthly Notices of the Royal Astronomical Society*, vol. 377, no. 1, pp. L64–L68, 2007.

[38] P. Ranalli, A. Comastri, and G. Setti, "The 2-10 keV luminosity as a star formation rate indicator," *Astronomy and Astrophysics*, vol. 399, no. 1, pp. 39–50, 2003.

[39] M. Salvato, O. Ilbert, G. Hasinger et al., "Dissecting photometric redshift for active galactic nucleus using *XMM*- and *Chandra*-cosmos samples," *Astrophysical Journal*, vol. 742, no. 2, article 61, 2011.